Journal of Metals, Materials and Minerals, 36(3), e2521, 2026

Surface characteristics of montmorillonite reinforced cellulose membranes derived from pineapple waste

Naufal Rizky AMASDA[1], Heru SURYANTO[1,2,*], Aminuddin AMINUDDIN[1], Uun YANUHAR[3], Nanda Lidya Cinta Aulia SARI[1], Agus SUYETNO[1], Komarudin KOMARUDIN[1], Fajar NUSANTARA[1], Gaguk JATISUKAMTO[4], and Aulia Surya RAMADHAN[5]

[1] *Department of Mechanical and Industrial Engineering, State University of Malang, Jl. Semarang, Malang, East Java, 65145, Indonesia*
[2] *Center of Science and Engineering (PSR), State University of Malang, Jl. Semarang, Malang, East Java, 65145, Indonesia*
[3] *Department of Aquatic Resources Management, Brawijaya University, Jl. Veteran, Malang, East Java, 65145, Indonesia*
[4] *Department of Mechanical Engineering, University of Jember, Jl. Kalimantan, Jember, East Java, 68124, Indonesia*
[5] *Study Program of Environmental Engineering, Brawijaya University, Jl. Veteran, Malang, East Java, 65145, Indonesia*

***Corresponding author e-mail**: heru.suryanto.ft@um.ac.id

Received date:
4 October 2025
Revised date:
17 November 2025
Accepted date:
1 April 2026

Keywords:
Bacterial cellulose;
BET analysis;
Membrane surface;
Montmorillonite;
Pineapple waste

Abstract

This study aims to investigate the effect of montmorillonite on the surface characteristics and porosity of bacterial nanocellulose (BNC) membranes derived from pineapple peel waste. The bacterial cellulose was synthesized using *Acetobacter xylinum* using pineapple peel extract as medium component. Bacterial nanocellulose membrane (BNC) was obtained by crushing and homogenizing bacterial cellulose in a high-pressure homogenizer. BNC membrane was reinforced with montmorillonite content of 2 wt% to 8 wt%. The membrane was characterized for its properties using SEM, FTIR, surface roughness tester, tensile tester, water holding capacity test, and BET analysis. The results showed that montmorillonite was well-dispersed within BNC matrix but exhibited agglomeration at higher concentrations. When the samples were analyzed using FTIR spectroscopy, observed changes in functional groups and molecular interactions at 2845 cm^{-1} Alkane C–H bond, confirming that components were successfully integrated. The surface roughness increased significantly from 28.33 ± 3.35 μm (control) to 82.23 ± 1.82 μm (8 wt% montmorillonite), confirming morphological change. The addition of montmorillonite has reduced the crystalline index and the mechanical properties of BNC membrane. BET analysis revealed a transition from microporous (1.6979 nm) to mesoporous structures (up to 2 nm) with enhanced surface area and pore diameter. Pore diameter and volume correlated with enhancing water holding capacity by 36.6% at montmorillonite content of 6 wt%. BC/montmorillonite membranes exhibit adjustable surface characteristics and porosity, thus providing potential for water treatment applications.

1. Introduction

In recent years, materials science and nanotechnology have risen rapidly, creating both opportunities for innovation and challenges for sustainable development [1]. In Indonesia, these fields have shown consistent growth, largely supported by the increasing use of composite materials from natural sources [2]. The development of nanocellulose-based membranes is of interest because many advanced features include high separation efficiency, low energy requirements, and potential for large-scale production [3]. Cellulose is known as the most abundant renewable biopolymer on Earth [4] that offers distinct structural characteristics and potential applications [5].

Bacterial cellulose (BC), as an environmentally friendly bio-polymer, has been utilized in various applications [6,7]. The advantages of BC for composite membranes due to its unique properties include a highly crystalline, mechanically robust, three-dimensional network of nanofibrils, and providing an optimal scaffold [8]. Different from cellulose from plants, BC is produced through microbial bio-fabrication using *Acetobacter xylinum*. These bacteria synthesize it from simple sugars such as D-glucose, forming an exopolysaccharide network on the surface of nutrient media. BC biosynthesis is an important process because the culture conditions tailor its structural and crystalline features, and enhance its performance for various applications [9].

The global population approaching 8 billion people causes demand for food to continue to increase, resulting in massive agricultural waste [10]. Pineapple processing is known to produce large amounts of peel waste, so it needs to be utilized as a sustainable source of nanocellulose [11]. Utilization of pineapple peel waste not only offers a cost-effective raw material but also supports the principle of a circular economy through valorization of agro-industrial by-products. The design of biomaterial nanostructures has become an effective strategy to improve functionality and expand its applications [12]. Many studies have developed BC-based nanocomposites reinforced with TiO_2, ZnO, Fe_3O_4, and graphite to improve their properties [13,14].

Nanoclay is a layered silicate nanomaterial that has potential as a composite reinforcement to improve mechanical, thermal, and barrier

properties [15]. Kaolinite and halloysite are types of nanoclay that have been used as reinforcing fillers in composites [16,17]. Montmorillonite, a kind of clay, has potential as a composite reinforcement due to its high aspect ratio [18] and typical cation exchange capacity [19], and high swelling capacity [20] compare to kaolinite. In addition to being composite reinforcement, montmorillonite has also been widely used as an adsorbent to remove various water pollutants, including heavy metals, organic contaminants, and pharmaceutical residues [21]. Its performance can be further enhanced when integrated into composite or adsorptive membranes, thereby improving removal efficiency [22].

It has been reported that combination of BC and montmorillonite resulted in robust nanocomposites with improved mechanical strength, thermal stability, and barrier properties [23]. The incorporation of montmorillonite into BC matrix generates a tortuous pathway for gas molecules, thereby reducing oxygen permeability and enhancing barrier performance [24]. Owing to these advantages, BC/montmorillonite nanocomposites have been explored in diverse sectors, including energy production, water treatment, food preservation, and biomedical applications [25]. However, only a few studies have investigated the development of BC membranes derived from pineapple peel waste, particularly regarding surface modification and porosity through montmorillonite reinforcement. Most existing research has focused on other nanoparticle additives, leaving the specific influence of montmorillonite on surface roughness, pore structure, and specific surface area largely underexplored. Therefore, the present study aims to investigate the effect of montmorillonite incorporation on bacterial nanocellulose (BNC) membranes synthesized from pineapple peel waste. The membranes were characterized in terms of surface morphology and porosity (SEM, roughness test, and Brunauer–Emmett–Teller analysis), chemical interactions (FTIR), X-ray diffraction (XRD), mechanical properties test, and water holding capacity (WHC).

2. Materials and methods

2.1 Materials

The pineapple peel waste was procured at a local market in Malang, East Java, Indonesia. The A.xylinum, a bacterium that produces cellulose, was obtained from the Laboratory of Applied Technology at Muhammadiyah University in Malang, Indonesia. The chemicals for cellulose production include ammonia, acetic acid, urea, sodium hydroxide, and glucose, which were purchased from Merck (Germany). Montmorillonite-type nanoclay containing 25 wt% to 30 wt% trimethyl stearyl ammonium was purchased from Sigma Aldrich (Singapore) with a mean particle size ≤ 20 μm.

2.2 Bacterial cellulose synthesis

Pineapple peel waste obtained from a local market was subjected to a cleaning process first to remove impurities. Subsequently, procedure for cellulose preparation was followed: 300 g of pineapple peel were blended at 25,000 revolutions per minute in a container with 2 liters of water to create the biowaste extract. The extract was then heated to 100°C, and 150 g of sugar, along with 5 g of urea, were added to the solution. 20% of the medium containing A.xylinum was added to the mix solution once it had cooled to 30°C. The fermentation process lasted for 10 days to 14 days, resulting in the production of BC/pellicle. The pellicle, which floated on the surface of the culture medium, was then harvested and collected for further processing.

2.3 Homogenization process

BNC extraction was done using a previously published procedure [26]. BC pellicles were cut into small fragments. To remove the impurities, the pellicle was immersed in 1% NaOH solution at 90°C for 2 h. After that, BC was rinsed with distilled water until the pH was neutral (pH 7). Fifty grams of pellicle were put in a blender container and added with a liter of distillate water and crushed for 5 min at 26,000 revolutions per minute. Subsequently, the colloid underwent five cycles of processing at a pressure of 150 bar using a high-pressure homogenizer (model AH-100D, Berkley Scientific, China). Afterward, it was filtered through Whatman No. 42 paper to isolate bacterial cellulose.

2.4 Synthesis of nanocomposite membrane

Ten grams of bacterial nanocellulose were stirred in 100 mL of demineralized water for 30 min. In a separate procedure, the required quantity of montmorillonite (at concentrations of 2 wt%, 4 wt%, 6 wt%, and 8 wt%) was combined with 100 mL of demineralized water and stirred for about 30 min. Once the montmorillonite is mixed, an ultrasonic treatment was applied with a 400 W, 20 kHz sonicator (UP-400S, Lawson Smarttech, China) through two successive 30 min treatments, resulting in a uniformly dispersed sample. Consequently, the mixtures of bacterial nanocellulose and montmorillonite were stirred for a further 30 min at 400 rpm. After that, the mixture undergoes vacuuming to remove bubbles from filaments, and then drying process was conducted in an oven at 60°C for 8 h.

2.5 Characterization

Morphological analysis was conducted using a Scanning electron microscope (FEI, Inspect-S50 type). During the SEM process, the sample films were cut into 10 mm × 10 mm sections and then coated with a thin layer of gold using a sputter coater (SC7-620 Emitech), and SEM was observed at a voltage of 15.00 kV with 5000x magnification.

FTIR analysis was utilized to observe functional group included in the BC/Montmorillonite nanocomposite membrane. The sample was cut with dimensions of 10 mm × 10 mm. FTIR spectra were recorded using the Shimadzu IR Prestige 21 (Japan) within wave number range of 400 cm^{-1} to 4000 cm^{-1} with a resolution of 4/cm.

The crystalline structure of membrane was observed by XRD equipment (PANalytical X'Pert Pro, Netherlands). The XRD scanning was conducted at 2θ from 10° to 60°. Crystalline index (CI) of the membrane was evaluated using the Segal equations (Equation (1)) [27].

$$CI = \frac{I_{(200)} - I_{(am)}}{I_{(200)}} \times 100\% \quad (1)$$

Where: $I_{(200)}$ is the intensity of the peak at 2θ about 22.5°; $I_{(am)}$ is the lowest intensity at 2θ about 18°.

Surface roughness and porosity were measured using a roughness tester and BET. The surface roughness of the BC membrane was measured using a surface roughness tester (SJ-301, Mitutoyo Co, Japan) with a 0.75 mN precision gauge. The horizontal and vertical roughness were measured at 200.0 μm·cm^{-1}, and 5.0 μm·cm^{-1}, respectively. Surface analysis using the BET instrument (Micromeritics, USA) was performed using nitrogen gas as the adsorbate. The samples were degassed for 4 h, and analysis was conducted at a bath temperature of –195°C.

Membrane tensile test was assessed according to the ASTM D638 V standard, using a tensile tester (TechnoLab, Indonesia) with a maximum load of 50 N. All samples were tested at a rate of 3 mm·min^{-1}, with five repetitions.

WHC of membranes was determined using a gravimetric method adapted from ASTM D570. A square specimen (10 mm × 10 mm) of membrane was oven-dried in an oven for 24 h at 50 ± 3°C to get dried mass (Mdry). Immerse the samples for 2 h in distilled water maintained at 23 ± 1°C. The immersion time of 2 h was selected based on preliminary tests showing that the water uptake reached equilibrium within this period. Upon stabilization, the wet samples were taken out of water, and the remaining surface water was carefully blotted using filter paper to get the wet mass (Mwet). WHC was determined using Equation (2).

$$M\ (\%) = \frac{M_{wet} - M_{dry}}{M_{dry}} \times 100 \qquad (2)$$

Quantitative data were statistically analyzed using a one-way ANOVA and Tukey's Honestly Significant Difference (HSD) test at a 0.05 significance level, in the Origin software (version 9).

3. Results and discussion

3.1 Surface morphology analysis

Morphology of BNC membrane after addition of montmorillonite is displayed in Figure 1. BC membrane without the addition of montmorillonite is shown in Figure 1(a). Following the addition of montmorillonite, clays are distributed as small surface aggregates within nanocomposite. Incorporation of montmorillonite alters the structure by forming intercalated nanocomposites. Additionally, SEM examination demonstrates that inclusion of montmorillonite alters surface morphology, suggesting a stronger interfacial interaction between montmorillonite and BNC matrix. As the content increases, montmorillonite starts to form slight aggregates, but remain evenly dispersed within BNC. Aggregation becomes more apparent with higher amounts of montmorillonite [28]. Agglomeration can happen because of the strong van der Waals forces among montmorillonite, which might lead to an uneven distribution within bacterial cellulose matrix and a reduction in effectiveness of nanocomposite properties [29].

3.2 FTIR analysis of BNC/Montmorillonite

The effect of montmorillonite incorporation on functional groups of bacterial cellulose membranes is shown in Figure 2. In pure bacterial cellulose membrane, the most intense band was observed at ~3350 cm^{-1}, corresponding to O–H stretching vibrations associated with abundant hydroxyl groups and adsorbed water molecules [30]. Upon montmorillonite addition, the intensity in this region increased, suggesting stronger hydrogen bonding interactions. This is consistent with nanoscale structure of clay, which generates hydroxyl groups at its fractured edges and facilitates additional interfacial interactions [31]. Other characteristic changes were also detected. The band near 1615 cm^{-1}, typically associated with C=C stretching in aromatic structures [32] and minor peak at 2134 cm^{-1} attributed to C≡C stretching of alkyne groups [33], remained visible, although with slight intensity variations after montmorillonite incorporation. A shift at ~750 cm^{-1} (aryl C–H bending) further indicates changes in molecular interactions between BC and montmorillonite. Notably, a new absorption peak emerged at 2845 cm^{-1}, corresponding to C–H stretching of alkanes, which may be related to hydrocarbon groups introduced during montmorillonite integration. These specific bands are attributed to alkyl chains in montmorillonite. Consistent with prior literature [34], incorporation of the same ammonium-modified montmorillonite resulted in detection of identical hydrocarbon peaks.

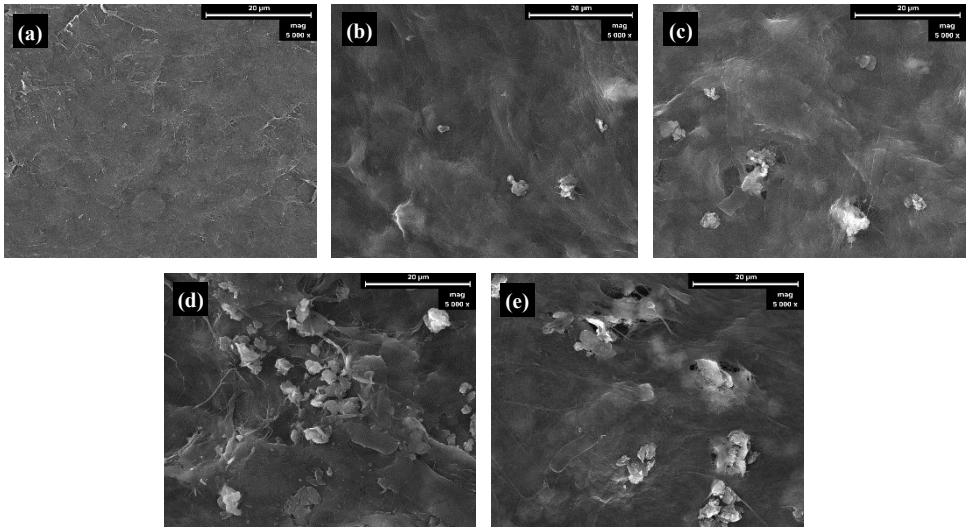

Figure 1. Morphology BNC montmorillonite: control (a), montmorillonite of 2 wt% (b), 4 wt% (c), 6 wt% (d),and 8 wt% (e).

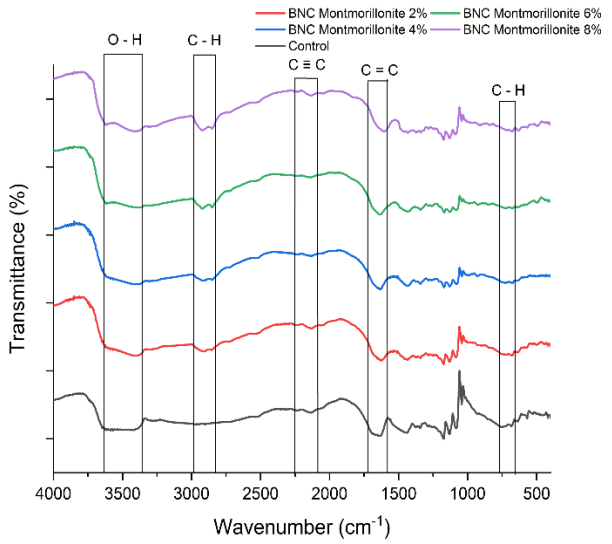

Figure 2. Transmittance BNC Montmorillonite.

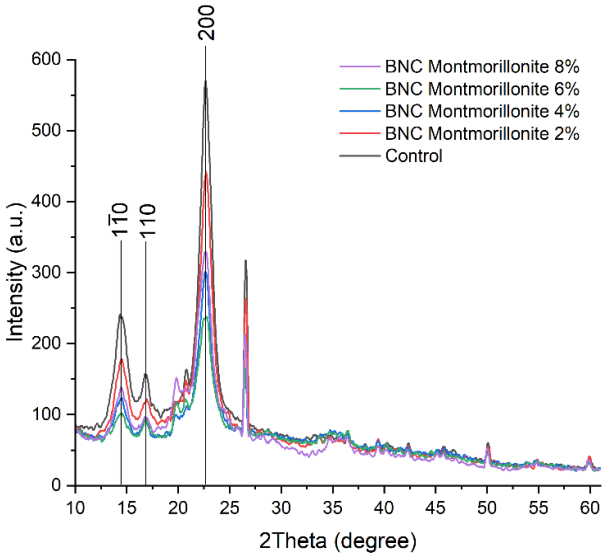

Figure 3. X-ray diffraction angle of BNC Montmorillonite.

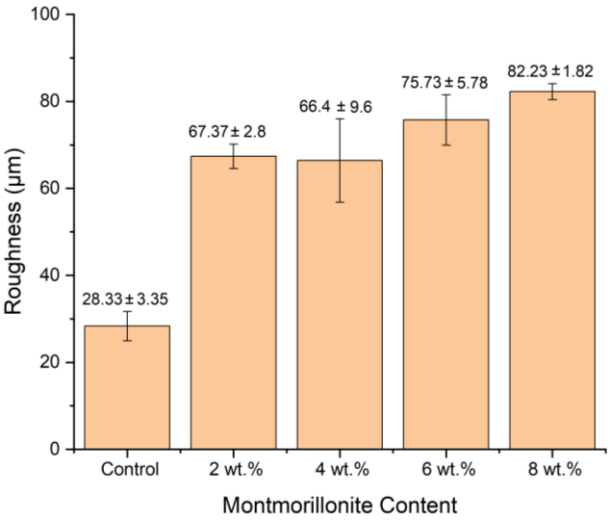

Figure 4. Surface roughness of BNC membrane with various montmorillonite contents.

3.3 Crystallinity analysis of BNC/Montmorillonite

The diffractogram of BNC nanocomposite membrane at different montmorillonite contents is depicted in Figure 3. All samples showed three diffraction peaks at 2θ of 14.4°, 16.8°, and 22.6° corresponds to $1\bar{1}0$, (110), and (200) lattice planes of cellulose type I structure [35]. Addition of montmorillonite reduced the peak intensity, especially at (200) plane. Quantification of CI indicates that control BNC membrane had the highest CI (82.9%) and declined with montmorillonite addition, with the lowest CI of 71.7% at 6 wt% montmorillonite content (Table 1). This observed reduction confirms successful intercalation of montmorillonite within cellulose network, which disrupted inherent hydrogen-bonding framework between fibrils [36]. This interaction consequently promoted formation of a more amorphous composite structure. This amorphous nature is favorable for water absorption as discussed in the subsequent section.

3.4 Surface roughness analysis of BNC/Montmorillonite

The surface roughness results of BNC/montmorillonite membranes are presented in Figure 4. To determine the overall membrane roughness, measurements were made at three randomly selected locations on each sample. Data show that adding montmorillonite increases surface roughness of bacterial cellulose: control (0 wt% montmorillonite) has a roughness of 28.33±3.35 μm, which sharply rises to 67.36±2.8 μm at 2 wt%. Although it decreases slightly to 66.40±9.6 μm at 4 wt%, surface roughness of membrane increases to 75.73±5.78 μm and 82.23±1.82 μm after being added by montmorillonite at 6 wt% and 8 wt%, respectively.

The increase in roughness was caused primarily by agglomeration of nanoparticles on membrane surface. Nanoparticles with a large surface area and high surface energy tend to aggregate, forming irregular topographies [37]. Differences in hydrophilic and hydrophobic properties can enhance this effect. BC derived from pineapple peel is highly hydrophilic due to abundant hydroxyl (–OH) groups that readily attract water, whereas montmorillonite is comparatively hydrophobic, consisting mainly of mineral particles that do not dissolve in water. This mismatch can reduce compatibility and promote surface aggregation [38].

The roughness values obtained in this work (28 μm to 82 μm) are significantly higher than those typically reported for bacterial cellulose composites, which often range from the nanometer to sub-micrometer scale. Suryanto *et al.* (2021) reported that film roughness is about 0.93 μm for BC films obtained from high-pressure homogenization [39]. Likewise, BC reinforced with graphite nanoplatelets showed roughness values between 1.14 μm and 2.48 μm depending on filler concentration [40]. Another study on dehydrated BC films reported roughness in the range of 81 nm to 195 nm, depending on drying method [41].

These comparisons suggest that the exceptionally high roughness observed in the present study is likely due to formation of larger surface agglomerates of montmorillonite, rather than nanoscale surface variations typically seen in BC composites. In filtration membranes, higher roughness is advantageous. Increased roughness promotes greater surface area and active sites, which can enhance water flux, adsorption capacity, and contaminant retention [42,43].

Table 1. Crystallinity Index of BNC/Montmorillonite.

Sample	2Theta of $I_{(200)}$ [°]	CI [%]
BNC control	22.6	82.9
BNC/Montmorillonite 2 wt%	22.6	79.5
BNC/Montmorillonite 4 wt%	22.5	76.4
BNC/Montmorillonite 6 wt%	22.5	71.7
BNC/Montmorillonite 8 wt%	22.4	74.3

Table 2. Mechanical properties of BNC/Montmorillonite.

Membrane	Tensile strength [MPa]	Elastic modulus [MPa]
BNC control	36.34 ± 0.74	49.98 ± 6.28
BNC/Montmorillonite 2 wt%	35.49 ± 0.20	26.69 ± 4.98
BNC/Montmorillonite 4 wt%	28.75 ± 0.40	17.96 ± 6.25
BNC/Montmorillonite 6 wt%	21.52 ± 0.27	18.54 ± 4.70
BNC/Montmorillonite 8 wt%	18.68 ± 0.04	25.66 ± 4.37

Thus, the elevated roughness observed in BNC/montmorillonite membranes indicates promising potential for water treatment and separation processes, particularly in applications requiring rapid adsorption kinetics and improved pollutant capture.

One-way ANOVA statistical analysis revealed that incorporation of montmorillonite into bacterial cellulose significantly affected surface roughness (n = 3, Pvalue = 0.000002, significance level = 0.05). ANOVA result confirmed a highly significant difference in Ra values across the different montmorillonite content. Further comparison using Tukey's HSD test showed that samples containing 4 wt%, 6 wt%, and 8 wt% montmorillonite exhibited significantly higher surface roughness than the control ($P < 0.001$), while 2 wt% montmorillonite sample did not differ significantly from the control ($P = 0.055$). Significant differences were also observed between higher montmorillonite content and lower ones, particularly between 8 wt% and 2 wt% (Pvalue = 0.0459).

3.5 Mechanical strength analysis of BNC/Montmorillonite

Mechanical properties of BNC/montmorillonite nanocomposite membrane are presented in Table 2. As a result, average ultimate tensile strength and elastic modulus decreased after the addition of montmorillonite. The average ultimate tensile strength remains stable from 36.34±0.74 MPa (control) to 35.49±0.2 MPa at 2 wt% montmorillonite. Subsequently, dropped to the lowest possible result was obtained at 8 wt% with a tensile strength of 18.68±0.04 MPa.

Statistical analysis using One-way ANOVA shows that montmorillonite content in membrane had a significant difference for both tensile strength ($F = 1165.51$, $P_{value} = 0.00$) and elastic modulus ($F = 17.67$, $P_{value} = 1.58 \times 10^{-4}$). Post-hoc Tukey's HSD analysis on tensile strength indicated that tensile strength differed significantly among all montmorillonite contents, but only non-significant comparison was between control and montmorillonite of 2 wt% ($P_{value} > 0.05$). The non-significant difference between the control and 2 wt% membrane suggests that a low montmorillonite content does not substantially disturb the native BNC nanofibrous network, so that the strength remains comparable to that of control membrane. Higher montmorillonite content (4 wt% to 8 wt%) promotes micro-aggregate formation and defects within BNC matrix, so it reduces tensile strength [39]. Instead of being evenly dispersed, montmorillonite likely clumps together, creating internal flaws. This disrupts matrix homogeneity and introduces weak spots [40]. Also, poor interfacial adhesion between montmorillonite and BNC is indicated by a decrease in elastic modulus. When interfacial bonds are weak, montmorillonite is unable to withhold loads effectively, resulting in a reduction in material stiffness [41,44].

For the elastic modulus, post-hoc Tukey's HSD analysis revealed that the control membrane as significantly different from all montmorillonite-containing membranes (2 wt% to 8 wt%) ($P_{value} < 0.05$). However, no significant differences were observed among the montmorillonite-treated groups themselves (2 wt%, 4 wt%, 6 wt%, and 8 wt%; $P_{value} > 0.05$). The presence of montmorillonite is sufficient to disrupt the highly ordered hydrogen-bonded BNC framework and shift the initial elastic response to a less rigid one. Further increases in montmorillonite from 2 wt% to 8 wt% resulted in only relatively small modulus changes compared to the experimental variability, so no additional significant differences were detected among the composite membranes. There was a slight increase in elastic modulus at 8 wt% montmorillonite content. Similar studies have reported that the addition of more montmorillonite tends to cause more excessive intercalation and agglomeration, which can degrade properties of material [45,46].

3.6 BET analysis of BNC/Montmorillonite

BET test results are presented as adsorption-desorption isotherm graphs as shown in Figure 5. All samples, from the control (0 wt% montmorillonite) to the highest montmorillonite content, exhibit type IV isotherms with hysteresis loops [45]. These loops are related to capillary condensation in the mesoporous structure (2 nm to 50 nm) and provide insight into pore geometry and surface interactions [38].

Table 3 shows that pure BNC membranes possessed an average pore diameter of 1.69 nm, consistent with a microporous structure. After montmorillonite addition, the pore size increased beyond 2 nm, indicating a transition to mesoporosity. This structural modification resulted in pore diameter increases of approximately 30% to 75% compared with the unmodified membrane. Although the numerical change in pore size may seem modest, the shift from micropores

Table 3. Specific surface area and pore distribution.

Membrane	Surface area [$m^2 \cdot g^{-1}$]	Pore diameter [nm]	Pore volume [$cm^3 \cdot g^{-1}$]
BNC control	2.8458	1.6979	0.0121
BNC/Montmorillonite 2 wt%	5.735	2.3959	0.0343
BNC/Montmorillonite 4 wt%	7.5203	2.2090	0.0467
BNC/Montmorillonite 6 wt%	6.4338	2.9694	0.0477
BNC/Montmorillonite 8 wt%	5.5229	2.9369	0.0405

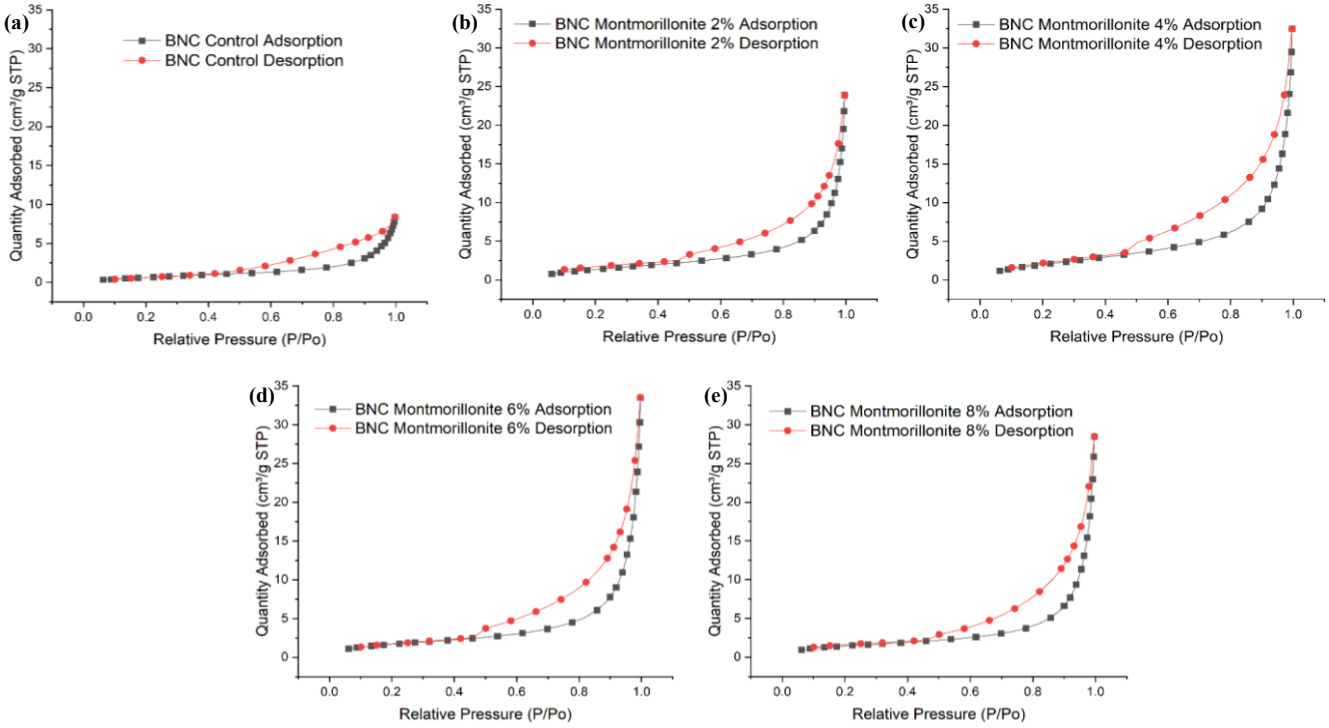

Figure 5. BET adsorption-desorption BNC membrane: control (a), montmorillonite of 2 wt% (b), 4 wt% (c), 6 wt% (d), and 8 wt% (e).

(<2 nm) to mesopores (>2 nm) is significant because it alters the functional behavior of membrane. Micropores typically offer high selectivity and strong adsorption affinity for small molecules and ions, while mesopores enhance diffusion, surface area, and pore volume, thereby facilitating faster mass transfer and higher adsorption capacity. The mesoporous characteristics observed in BNC membranes with 2 wt% to 8 wt% montmorillonite are therefore advantageous for applications requiring rapid interaction kinetics and greater molecular accommodation, such as pollutant adsorption and separation processes [47]. This transition highlights the dual role of montmorillonite: reinforcing BC matrix and tuning its porosity into mesoporous regime. These results may indicate the potential of this membrane to be more suitable for practical water treatment applications compared to pure BC structures.

Similar reports indicate that porosity is also increased due to presence of ZnO nanoparticles in BC [48]. This increased porosity leads to improved adsorption performance. The mesoporous structure, in particular, is advantageous because it accelerates diffusion of adsorbate molecules and allows the capture of larger or more complex contaminants. In the case of BNC/montmorillonite membranes, the transition from a microporous to a mesoporous structure shows higher potential for pollutant adsorption and separation applications. However, finding an optimal balance between porosity and structural stability is crucial, as excessive porosity can compromise mechanical integrity and selectivity. Therefore, structural modifications not only affect adsorption performance but can also influence barrier properties, as pore size and distribution are directly related to gas permeability [49].

3.7 Water holding capacity

WHC membrane was tested and the result is shown in Figure 6. Control BNC membrane has WHC value of 66.59±9.21% then decreased to 50.62±4.05% after the addition of 2 wt% montmorillonite. The exfoliation of montmorillonite platelet is thought to be a barrier to water adsorption. These platelet limit mobility of cellulose chains and minimize water penetration, as well as increasing dimensional stability of membrane [50]. At montmorillonite content of 6 wt%, WHC of membrane had a maximum value of 90.99±19.35% or an increase of 36.6% compared to the control membrane. Increasing water adsorption of membrane suggest due to increase in pore size and volume as confirmed by BET results. In addition, montmorillonite itself contributes to increase membrane hydrophilicity, thus attracting more water molecules into matrix [51]. At the highest montmorillonite content (8 wt%), WHC decreased to 72.3±15.78%. This indicates that abundant montmorillonite content can cause pore clogging, as the additional clay content fills the gaps and inhibits water passage [52].

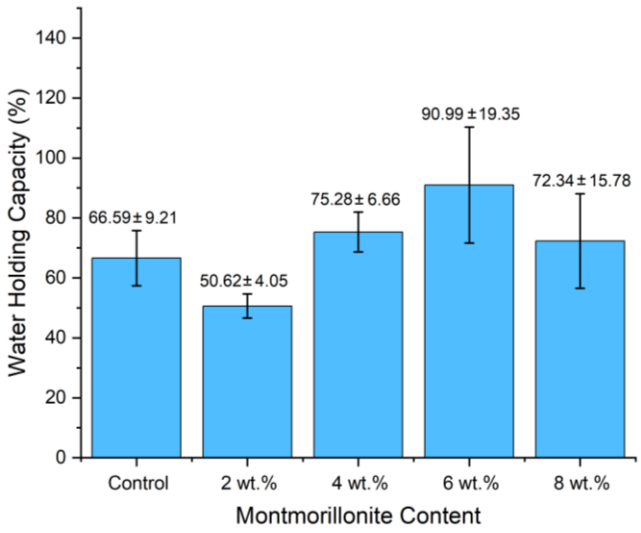

Figure 6. Water holding capacity of BNC/montmorillonite membrane.

Statistical analysis using One-way ANOVA confirmed that WHC was significantly affected by differences in montmorillonite content ($F = 4.17$, $Pvalue = 0.0306$). Tukey test showed that only 6 wt% group differed significantly from 2 wt% group. This suggests that a montmorillonite content of 6 wt% is high enough to substantially increase the number of hydrophilic sites and effective free volume within BNC network. At lower content (2 wt%), the amount of clay is likely insufficient to induce great structural and interfacial changes, whereas at higher content (8 wt%) particle aggregation and partial pore blocking may counterbalance the additional hydrophilic surface, resulting in WHC values that are not statistically different from the other groups.

4. Conclusions

Bacterial nanocellulose (BNC) membranes with varying montmorillonite content (0 wt% to 8 wt%) were successfully fabricated and characterized. FTIR spectra confirmed emergence of a new C–H stretching peak at 2845 cm^{-1}, indicating chemical interactions between montmorillonite and BC matrix. The addition of montmorillonite to membrane caused aggregation of montmorillonite on the surface, thus changing the membrane morphology. The addition of montmorillonite to membrane caused a decrease in crystallinity index from 82.9% to 74.3% (8 wt%). This was presumably due to intercalation of montmorillonite plates that disrupted cellulose framework. Surface roughness value increased with the addition of montmorillonite, indicating greater surface heterogeneity. The formation of micro-aggregates reduces tensile strength from 36.34±0.74 (control) MPa to 18.68±0.04 (8 wt% montmorillonite). Addition of montmorillonite to membrane causes a transition from a microporous (1.69 nm) to a mesoporous (2.39 nm to 2.97 nm) structure. Pore diameter also increases by ranging from 30% to 75% compared with the unmodified membrane. This increase in porosity correspond to 36.6% increase in water holding capacity. These findings indicate that BNC/montmorillonite membrane derived from pineapple waste can be used as a candidate membrane for water treatment applications. However, further research on its barrier properties, chemical stability, and long-term operation is needed to fully validate its practical use.

Acknowledgements

We would like to express our deepest gratitude to the LPPM of State University of Malang for their support and funding through Penelitian Unggulan Pusat scheme program with contract number 4.4.796/UN32.14.1/LT/2024.

References

[1] M. N. Norizan, S. S. Shazleen, A. H. Alias, F. A. Sabaruddin, M. R. M. Asyraf, E. S. Zainudin, N. Abdullah, M. S. Samsudin, S. H. Kamarudin, and M. N. F. Norrrahim, "Nanocellulose-based nanocomposites for sustainable applications: A review," *Nanomaterials*, vol. 12, no. 19, p. 3483, 2022.

[2] R. Raharjo, T. Dwi Widodo, R. Bintarto, and F. A. Alamsyah, "Characterization of bamboo petung fiber reinforced composites with environmentally friendly enzymes," *Journal of Mechanical Engineering Science and Technology*, vol. 9, no. 1, pp. 165–176, 2025.

[3] S. S. Jaffar, S. Saallah, M. Misson, S. Siddiquee, J. Roslan, S. Saalah, and W. Lenggoro, "recent development and environmental applications of nanocellulose-based membranes," *Membranes*, vol. 12, no. 3, p. 287, 2022.

[4] Y. Y. Li, B. Wang, M. G. Ma, and B. Wang, "Review of recent development on preparation, properties, and applications of cellulose-based functional materials," *International Journal of Polymer Science,* vol. 2018, p. 8973643, 2018.

[5] H. Rostamabadi, Y. Bist, Y. Kumar, M. Yildirim-Yalcin, T. Ceyhan, and S. R. Falsafi, "Cellulose nanofibers, nanocrystals, and bacterial nanocellulose: Fabrication, characterization, and their most recent applications," *Future Postharvest and Food*, vol. 1, no. 1, pp. 5–33, 2024.

[6] P. Cazón, and M. Vázquez, "Bacterial cellulose as a biodegradable food packaging material: A review," *Food Hydrocolloids*, vol. 113, p. 106530, 2021.

[7] L. Popa, M. V. Ghica, E. E. Tudoroiu, D. G. Ionescu, and C. E. Dinu-Pîrvu, "Bacterial cellulose—A remarkable polymer as a source for biomaterials tailoring," *Materials*, vol. 15, no. 3, p. 1054, 2022.

[8] P. Samyn, A. Meftahi, S. A. Geravand, M. E. M. Heravi, H. Najarzadeh, M. S. K. Sabery, and A. Barhoum, "Opportunities for bacterial nanocellulose in biomedical applications: Review on biosynthesis, modification and challenges," *International Journal of Biological Macromolecules*, vol. 231, p. 123316, 2023.

[9] A. H. Tayeb, E. Amini, S. Ghasemi, and M. Tajvidi, "Cellulose nanomaterials-binding properties and applications: A review," *Molecules*, vol. 23, no. 10, p. 2684, 2018.

[10] A. F. Alphanoda, E. A. Pane, A. Riyanto, and A. A. Permanasari, "The role of banana peel surface pores through increasing temperature for efficient hydrogen production," *Journal of Mechanical Engineering Science and Technology*, vol. 8, no. 2, pp. 421–433, 2024.

[11] W. Ben Mbarek, L. Escoda, J. Saurina, E. Pineda, F. M. Alminderej, M. Khitouni, and J. J. Suñol, "Nanomaterials as a

sustainable choice for treating wastewater: A review," *Materials*, vol. 15, no. 23, p. 8576, 2022.

[12] S. Nitodas, M. Skehan, H. Liu, and R. Shah, "Current and potential applications of green membranes with nanocellulose," *Membranes*, vol. 13, no. 8, p. 694, 2023.

[13] U. Yanuhar, H. Suryanto, S. A. Sardjono, I. K. Ningrum, A. Aminnudin, and J. S. Binoj, "Effect of titanium dioxide nanoparticle on properties of nanocomposite membrane made of bacterial cellulose," *Journal of Natural Fibers*, vol. 19, no. 16, pp. 13914–13927, 2022.

[14] M. Fariz Nafiir, Sudirman, E. Yuanita, S. E. Arshad, R. A. Lusiana, and M. Ulfa, "Synthesis and characterization of bacterial cellulose composite with graphite and TiO_2-ZnO: Structural and functional analysis," *Acta Chimica Asiana*, vol. 7, no. 2, pp. 478–486, 2024.

[15] P. Nehra, and R. P. Chauhan, "Eco-friendly nanocellulose and its biomedical applications: current status and future prospect," *Journal Biomaterial Science, Polymer Edition*, vol. 32, no. 1, pp. 112–149, 2021.

[16] L. W. Wong, and J. B. L. Tan, "Halloysite nanotube-polymer nanocomposites: A review on fabrication and biomedical applications," *Journal of Manufacturing Processes*, vol. 118, pp. 76–88, 2024.

[17] S. P. Bangar, V. Chaudhary, S. Khubber, and W. S. Whiteside, "Kaolinite-based nanocomposites for enhancing starch and other biodegradable polymer applications in food packaging," *International Journal of Biological Macromolecules*, vol. 320, p. 145889, 2025.

[18] J. Xu, L. Cheng, Z. Zhang, L. Zhang, C. Xiong, W. Huang, Y. Xie, and L. Yang, "Highly exfoliated montmorillonite clay reinforced thermoplastic polyurethane elastomer: In situ preparation and efficient strengthening," *RSC Advances*, vol. 9, no. 15, pp. 8184–8196, 2019.

[19] H. Yan, and Z. Zhang, "Effect and mechanism of cation species on the gel properties of montmorillonite," *Colloids and Surfaces A: Physicochemical and Engineering Aspects*, vol. 611, p. 125824, 2021.

[20] S. Amiri, A. Esfandyari Bayat, and S. Akbari, "Swelling characteristics of various clays in presence of an aqueous environment under different conditions," *Colloids and Surfaces A: Physicochemical and Engineering Aspects*, vol. 707, p. 135942, 2025.

[21] N. S. Aljohani, Y. N. Kavil, R. K. Al-Farawati, S. Saad Alelyani, M. I Orif, Y. A. Shaban, S. R. Al-Mhyawi, E. H. Aljuhani, and M. Abdel Salam, "The effective adsorption of arsenic from polluted water using modified Halloysite nanoclay," *Arabian Journal of Chemistry*, vol. 16, no. 5, p. 104652, 2023.

[22] M. N. Subramaniam, P. S. Goh, W. J. Lau, and A. F. Ismail, "The roles of nanomaterials in conventional and emerging technologies for heavy metal removal: A state-of-the-art review," *Nanomaterials*, vol. 9, no. 4, p. 625, 2019.

[23] M. Ö. Seydibeyoğlu, A. Dogru, J. Wang, M. Rencheck, Y. Han, L. Wang, E. A. Seydibeyoğlu, X. Zhao, K. Ong, J. A. Shatkin, S. Shams Es-haghi, S. Bhandari, S. Ozcan, and D. J. Gardner, "Review on hybrid reinforced polymer matrix composites with nanocellulose, nanomaterials, and other fibers," *Polymers*, vol. 15, no. 4, p. 984, 2023.

[24] K. Y. Perera, M. Hopkins, A. K. Jaiswal, and S. Jaiswal, "Nanoclays-containing bio-based packaging materials: Properties, applications, safety, and regulatory issues," *Journal of Nanostructure Chemical*, vol. 14, no. 1, pp. 71–93, 2024.

[25] C. Sharma, R. Dhiman, N. Rokana, and H. Panwar, "Nanotechnology: An untapped resource for food packaging," *Frontiers in Microbiology*, vol. 8, p. 1735, 2017.

[26] N. R. Amasda, H. Suryanto, U. Yanuhar, F. Nusantara, and Q. Alief Sias, "Surface analysis of bacterial cellulose membrane made from biowaste added with ZnO nanopowder," *Journal of Mechanical Engineering Science and Technology*, vol. 9, no. 1, pp. 281–290, 2025.

[27] L. Segal, J. J. Creely, A. E. Martin, and C. M. Conrad, "An empirical method for estimating the degree of crystallinity of native cellulose using the X-ray diffractometer," *Textile Research Journal*, vol. 29, no. 10, pp. 786–794, 1959.

[28] B. N. Jung, H. W. Jung, D. Kang, G. H. Kim, and J. K. Shim, "Synergistic effect of cellulose nanofiber and nanoclay as distributed phase in a polypropylene based nanocomposite system," *Polymers*, vol. 12, no. 10, pp. 1–15, 2020.

[29] I. A. Borojeni, A. Jenab, M. Sanjari, C. Boudreault, M. Klinck, S. Strong, and A. R. Riahi, "Effect of nanoclay addition on the morphology, fiber size distribution and pore size of electrospun polyvinylpyrrolidone (Pvp) composite fibers for air filter applications," *Fibers*, vol. 9, no. 8, p. 48, 2021.

[30] H. Suryanto, S. Sukarni, Y. Rohmat, A. Pradana, U. Yanuhar, and K. Witono, "Effect of mercerization on properties of mendong (Fimbristylis globulosa) fiber," *Songklanakarin Journal of Science and Technology*, vol. 41, no. 3, pp. 624–630, 2019.

[31] S. B. Y. Abeywardena, S. Perera, K. M. Nalin de Silva, and N. P. Tissera, "A facile method to modify bentonite nanoclay with silane," *International Nano Letter*, vol. 7, no. 3, pp. 237–241, 2017.

[32] P. Wongsa, P. Phatikulrungsun, and S. Prathumthong, "FT-IR characteristics, phenolic profiles and inhibitory potential against digestive enzymes of 25 herbal infusions," *Scientific Reports*, vol. 12, no. 1, p. 6631, 2022.

[33] A. B. D. Nandiyanto, R. Oktiani, and R. Ragadhita, "How to read and interpret ftir spectroscope of organic material," *Indonesian Journal of Science and Technology*, vol. 4, no. 1, pp. 97–118, 2019.

[34] C. Cojocaru, P. Pascariu, A. C. Enache, A. Bargan, and P. Samoila, "Application of surface-modified nanoclay in a hybrid adsorption-ultrafiltration process for enhanced nitrite ions removal: Chemometric approach vs. machine learning," *Nanomaterials*, vol. 13, no. 4, p. 697, 2023.

[35] T. Rosén, H. He, R. Wang, C. Zhan, S. Chodankar, A. Fall, C. Aulin, P. T. Larsson, T. Lindström, and B. S. Hsiao, "Cross-sections of nanocellulose from wood analyzed by quantized polydispersity of elementary microfibrils," *ACS Nano*, vol. 14, no. 12, pp. 16743–16754, 2020.

[36] A. Olszewski, A. Ławniczak, P. Kosmela, M. Strąkowski, A.

Mielewczyk-Gryń, A. Hejna, and Ł. Piszczyk, "Influence of surface-modified montmorillonite clays on the properties of elastomeric thin layer nanocomposites," *Materials*, vol. 16, no. 4, p. 1703, 2023.

[37] K. Muralishwara, Y. N. Sudhakar, U. A. Kini, S. Sharma, and B. M. Gurumurthy, "Moisture absorption and spectroscopic studies of epoxy clay nanocomposite," *Polymer Bulletin*, vol. 79, no. 7, pp. 5587–5611, 2022.

[38] C. Li, Q. Li, X. Ni, G. Liu, W. Cheng, and G. Han, "Coaxial electrospinning and characterization of core-shell structured cellulose nanocrystal reinforced PMMA/PAN composite fibers," *Materials*, vol. 10, no. 6, p. 572, 2017.

[39] V. Sorkin, Q. X. Pei, P. Liu, W. Thitsartarn, C. B. He, and Y. W. Zhang, "Atomistic-scale analysis of the deformation and failure of polypropylene composites reinforced by functionalized silica nanoparticles," *Scientific Reports*, vol. 11, no. 1, p. 23108, 2021.

[40] Z. F. Merzah, S. Fakhry, T. G. Allami, N. Y. Yuhana, and A. Alamiery, "Enhancement of the properties of hybridizing epoxy and nanoclay for mechanical, industrial, and biomedical applications," *Polymers*, vol. 14, no. 3, p. 526, 2022.

[41] M. C. Gowrishankar, M. Shettar, P. Somdee, N. Rangaswamy, and G. R. Chate, "A review on mechanical, water-soaking, thermal, and wear properties of nanoclay-polyester nanocomposites," *Discover Materials*, vol. 5, no. 1, p. 105, 2025.

[42] Y. Ibrahim, and N. Hilal, "A critical assessment of surface-patterned membranes and their role in advancing membrane technologies," *ACS ES&T Water*, vol. 3, no. 12, pp. 3807–3834, 2023.

[43] L. S. Azmi, N. 'Ain Jabit, S. Ismail, K. E. H. Ku Ishak, and T. K. Abdullah, "Membrane filtration technologies for sustainable industrial wastewater treatment: A review of heavy metal removal," *Desalination Water Treatment*, vol. 323, p. 101321, 2025.

[44] Y. Zare, "Effects of imperfect interfacial adhesion between polymer and nanoparticles on the tensile modulus of clay/polymer nanocomposites," *Applied Clay Science*, vol. 129, pp. 65–70, 2016.

[45] M. N. Uddin, M. T. Hossain, N. Mahmud, S. Alam, M. Jobaer, S. I. Mahedi, and A. Ali, "Research and applications of nanoclays: A review," *SPE Polymers*, vol. 5, no. 4, pp. 507–535, 2024.

[46] N. L. C. A. Sari, A. Aminnudin, H. Suryanto, J. S. Binoj, B. M. Bright, G. Jatisukamto, H. W. Wijaya, A. F. Osman, and U. Yanuhar, "Characteristics of membranes derived from pineapple biowaste: the effect of nanoclay addition," *Applied Science and Engineering Progress*, vol. 19, no. 1, pp. 1–13, 2025.

[47] A. Kondor, A. Santmarti, A. Mautner, D. Williams, A. Bismarck, and K. Y. Lee, "On the BET surface area of nanocellulose determined using volumetric, gravimetric and chromatographic adsorption methods," *Frontiers in Chemical Engineering*, vol. 3, p. 738995, 2021.

[48] L. Wu, Y. Li, Z. Fu, and B. L. Su, "Hierarchically structured porous materials: Synthesis strategies and applications in energy storage," *National Science Review*, vol. 7, no. 11, pp. 1667–1701, 2020.

[49] J. Zhu, R. Zhang, Y. Zhang, and F. He, "The fractal characteristics of pore size distribution in cement-based materials and its effect on gas permeability," *Scientific Reports*, vol. 9, no. 1, p. 17191, 2019.

[50] L. Solhi, V. Guccini, K. Heise, I. Solala, E. Niinivaara, W. Xu, K. Mihhels, M. Kröger, Z. Meng, J. Wohlert, H. Tao, E. D. Cranston, and E. Kontturi, "Understanding nanocellulose-water interactions: Turning a detriment into an asset," *Chemical Reviews*, vol. 123, no. 5, pp. 1925–2015, 2023.

[51] N. A. Burger, B. Loppinet, A. Clarke, and G. Petekidis, "How preparation protocols control the rheology of organoclay gels," *Industrial and Engineering Chemistry Research*, vol. 64, no. 13, pp. 6980–6991, 2025.

[52] L. Xing, L. Huang, Y. Yang, J. Xu, W. Zhang, G. Chi, and X. Hou, "The blocking effect of clay in groundwater systems: A case study in an Inland plain area," *International Journal of Environmental Research and Public Health*, vol. 15, no. 9, p. 1816, 2018.